

# The gamma-ray visibility of supernova remnants

## A test of cosmic ray origin

L. O'C. Drury<sup>1</sup>, F. A. Aharonian<sup>2</sup> and H. J. Völk<sup>2</sup>

<sup>1</sup> Dublin Institute for Advanced Studies, School of Cosmic Physics, 5 Merrion Square, Dublin 2, Ireland

<sup>2</sup> Max-Planck-Institut für Kernphysik, Postfach 103980, W-6900 Heidelberg-1

Received .....; accepted .....

**Abstract.** Recent calculations of particle acceleration in supernova remnants (SNRs) are used to estimate the associated  $\gamma$ -ray production. For source spectra which are power-laws in momentum (or rigidity) the production efficiency of  $\gamma$ -rays with energy  $E_\gamma > 100$  MeV is shown to be about a factor 2–3 lower than the value conventionally used for the interstellar medium and to depend only weakly on the spectral index of the power-law (in the range expected). Because the energy transferred to accelerated particles is rather tightly constrained by the total Galactic cosmic ray power, if SNRs are the main source of Galactic cosmic rays, this leads to an almost model-independent prediction of the SNR  $\gamma$ -ray luminosity in the band  $E_\gamma > 100$  MeV.

A detailed discussion of instrumental sensitivities and backgrounds shows that detection of SNRs in the  $E_\gamma > 100$  MeV band with, for example, the Energetic Gamma Ray Experiment Telescope (EGRET) will be difficult, but should not be impossible. However, and significantly, the prospects look much better in the TeV band accessible to modern imaging atmospheric Cherenkov telescopes. It should be possible to detect SNRs out to distances of 10 kpc if the region of the ISM into which they are expanding has a high enough density ( $n > 0.1 \text{ cm}^{-3}$ ) so that their  $\gamma$ -ray luminosity is high enough.

Finally, it is pointed out that existing and planned airshower arrays can place important limits on the extension of the accelerated particle spectra in SNRs to energies above 100 TeV. In conjunction with spectral measurements in the TeV region and detections or upper limits in the 100 MeV band this could provide a crucial test of current theories of particle acceleration in SNRs.

**Key words:** Gamma-rays – Cosmic ray origin – supernova remnants

### 1. Introduction

There is no clear observational proof that the nuclear component of cosmic rays is produced in supernova remnants (SNRs) although this is widely believed, at least for particle energies less than about  $10^{14}$  eV per nucleon. This general conviction

is mainly based on two facts; first, that a theoretical acceleration mechanism exists with certain attractive properties (diffusive shock acceleration: two recent reviews which emphasise the astrophysical applications are Blandford and Eichler, 1987; Berezhko and Krymsky, 1988), and secondly, that the galactic SNaE (and thus the resultant SNRs) are almost the only known potential sources with the necessary amount of available energy. Although plausible, these are indirect and unsatisfactory arguments. It is clearly desirable to seek direct evidence for accelerated nuclei in SNRs. The best hope would appear to be gamma-ray observations. Indeed some thirty years ago it was this, in the context of cosmic ray sources in general rather than SNRs in particular, which was at the heart of the rationale for missions like SAS-II and COS-B. If the nuclear component of the cosmic rays is strongly enhanced inside SNRs, then through nuclear collisions leading to pion production and subsequent decay,  $\gamma$ -rays will inevitably be produced<sup>1</sup>. In this paper we discuss some estimates of the  $\gamma$ -ray visibility of SNRs in the energy range around 100 MeV typical of the EGRET instrument on the Compton Observatory, the TeV energy range accessible to ground-based Cherenkov telescopes and the range above 10 TeV which can be covered by modern airshower arrays.

Diffusive shock acceleration, as applied to cosmic ray production in SNRs has been studied by many authors (eg Blandford and Ostriker, 1980; Krymsky and Petukhov, 1981; Prischep and Ptuskin, 1981; Bogdan and Völk, 1983; Moraal and Axford, 1983; Lagage and Cesarsky, 1983; Jokipii and Ko, 1987; Berezhko and Krymsky, 1988; Völk, Zank and Zank, 1988; Dorfi, 1990; Kang and Jones, 1991). In general, it must be said that all calculations contain *ad hoc* parametrizations of various aspects of the physics, especially the injection of particles into the acceleration process. Recent comparisons (Kang and Drury, 1992) show that the 'simplified models' (Drury, Markiewicz and Völk, 1989 [DMV]; Markiewicz, Drury and Völk 1990) are good approximations to the much more detailed hydrodynamical calculations, and in particular that the

<sup>1</sup> There will also be Bremsstrahlung and Inverse Compton components, produced by the electrons, both primary (directly accelerated) and secondary (from  $\pi^\pm$  decays), known from radio synchrotron observations to be present in SNRs. By considering only the gamma rays of hadronic origin we obtain a lower bound to the overall  $\gamma$ -ray emission of SNRs.

differences (in the worst cases factors of order two in the energy densities) are less than the uncertainties in the parametrizations of the underlying physics. This suggests that they can be used to obtain estimates of the gamma-ray flux to be expected from nuclear interactions in a SNR.

It is important to note that although the injection rate has to be specified in an essentially arbitrary fashion, the overall rate is rather tightly constrained by the observationally inferred energy requirements. When allowance is made for the energy-dependent escape of particles above a few GeV (Swordy et al, 1990) the traditional estimates of production efficiency are raised from a few percent to something above 10% per supernova (Völk et al, 1985; DMV) if the bulk of the cosmic ray nuclei are indeed accelerated in SNRs.

## 2. Expected $\gamma$ -ray fluxes

In the simplified models the SNR is divided into three regions: an interior region filled with hot gas and accelerated particles but very little mass, an immediate post shock region where most of the matter is concentrated, and a shock precursor region where the accelerated particles diffusing ahead of the shock compress the ambient medium. In each of these regions we know the energy density of the accelerated cosmic ray particles and the mass density. The production rate of  $\gamma$ -rays per unit volume can be written as

$$Q_\gamma = \mathcal{E}_\gamma n = q_\gamma n E_C \quad (1)$$

where  $n$  is the number density of the gas,  $E_C$  is the CR energy density and  $q_\gamma$  is the  $\gamma$ -ray emissivity normalized to the CR energy density,  $q_\gamma = \mathcal{E}_\gamma/E_C$ . For the galactic CR in the diffuse interstellar medium (ISM), outside sources, the  $\gamma$ -ray emissivity above 100 MeV due to nuclear collisions is about  $\mathcal{E}_\gamma(\geq 100 \text{ MeV}) \approx (1 - 1.5) \times 10^{-25} \text{ s}^{-1}(\text{H-atom})^{-1}$  (e.g. Stecker, 1971; Dermer, 1986) and  $E_C \approx 10^{-12} \text{ erg cm}^{-3}$ . The corresponding  $q_\gamma(\geq 100 \text{ MeV}) \approx 10^{-13} \text{ s}^{-1} \text{ erg}^{-1} \text{ cm}^3(\text{H-atom})^{-1}$  in the ISM can also be used for rough estimates of the  $\gamma$ -ray luminosity of SNRs (see below).

In fact, because the spectrum in the source is expected to be harder than the observed cosmic ray spectrum (which we know, from the energy dependence of the relative abundance of spallation products, to have been softened by propagation effects; Juliusson et al, 1972) this is almost certainly an overestimate of the production rate in SNRs. The spatially averaged spectrum in the source is probably of the form  $f(p) \propto p^{-\alpha}$  with  $4 \leq \alpha \leq 4.3$ , whereas the observed cosmic ray spectrum has  $\alpha \approx 4.7$ . Gamma rays above 100 MeV are produced by particles of energy above about 1 GeV per nucleon and the cross-sections are not very energy-dependent; thus the gamma production rate may be taken to be proportional to the number density of relativistic particles. For a given energy density, the harder the spectrum the lower will be the total number density of particles. On the other hand, if the spectrum extends to energies below about 1 GeV per nucleon, a harder spectrum will have fewer particles which contribute to the total energy density but do not generate observable  $\gamma$ -rays. To quantify these competing effects let us, following DMV, consider a simple power-law spectrum of the form

$$f(p) = f_0(p/2mc)^{-\alpha} \quad (2)$$

where  $f$  is the (isotropic) phase space density and  $p$  is momentum with a lower cut-off at  $p_{\text{inj}}$  and an upper cut-off at  $p_{\text{max}}$ . Then the number density of relativistic particles with  $p > 2mc$  is easily calculated to be

$$N_R = \frac{1}{\alpha - 3} 4\pi f_0 (2mc)^3 \left[ 1 - \left( \frac{p_{\text{max}}}{mc} \right)^{3-\alpha} \right] \quad (3)$$

and for  $\alpha \geq 4$  and  $p_{\text{max}} \gg mc$  the dependence on the upper cut-off can be neglected. On dividing by the corresponding energy density (as calculated in DMV) we obtain

$$\begin{aligned} \frac{N_R}{E_C} &= \frac{1}{2mc^2} \left[ 1 - \frac{p_{\text{inj}}}{2mc} + \ln \left( \frac{p_{\text{max}}}{2mc} \right) \right]^{-1}, & \alpha = 4, \\ &= \frac{1}{2(\alpha - 3)mc^2} \left[ \frac{1 - (p_{\text{inj}}/2mc)^{5-\alpha}}{5-\alpha} \right. \\ &\quad \left. + \frac{(p_{\text{max}}/2mc)^{4-\alpha} - 1}{4-\alpha} \right]^{-1}, & 4 < \alpha < 5, \\ &= \frac{1}{4mc^2} \left[ \ln \left( \frac{2mc}{p_{\text{inj}}} \right) + 1 - \frac{2mc}{p_{\text{max}}} \right]^{-1}, & \alpha = 5. \end{aligned} \quad (4)$$

It is easy to see that for typical values of  $p_{\text{inj}}/mc \approx 10^{-3} - 10^{-2}$  and  $p_{\text{max}}/mc \approx 10^5 - 10^6$  the ratio  $N_R/E_C$  is rather independent of  $\alpha$  even in the most extreme case of a hard source spectrum proportional to  $p^{-4}$  and an ambient spectrum of the form  $p^{-4.7}$ . This semi-quantitative argument is confirmed by numerical calculations which show that for the spectrum of accelerated particles represented by Eq. (2) the production rate is almost independent of the spectral index  $\alpha$ . In fact, for  $4.1 \leq \alpha \leq 4.7$  the production rate may be considered constant within 20% (see Table 1) of

$$q_\gamma(\geq 100 \text{ MeV}) \approx 0.5 \times 10^{-13} \text{ s}^{-1} \text{ erg}^{-1} \text{ cm}^3(\text{H-atom})^{-1} \quad (5)$$

which is a factor of three less than the corresponding value for a Galactic CR flux of the form  $J_p(E) \propto (E + mc^2)^{-2.75}$  where  $E$  is kinetic energy. This particular form for the spectrum gives a very high (close indeed to the maximum possible) efficiency for the production of  $\geq 100 \text{ MeV}$   $\gamma$ -rays (at fixed CR energy density) since it contains negligible energy density in nonrelativistic particles (useless for gamma production) and, as mentioned above, at the same time has a low energy density for particles with energy much above a few GeV. As the  $\pi^0$ -production cross-section becomes constant above a few GeV the maximum value is reached in the case of a monoenergetic beam of protons with energy 1–2 GeV. The results of numerical calculations of  $q_\gamma(\geq 100 \text{ MeV})$  for different spectral indices  $\alpha$  are presented in Table 1.

At energies  $E \gg 100 \text{ MeV}$  the production spectrum of  $\gamma$ -rays reproduces the spectral shape of the distribution of parent protons. The emissivity,  $\mathcal{E}_\gamma$ , for power-law spectra of relativistic protons can be presented in a simple analytic form (Appendix A). In the case of a source spectrum of the form given in Eq. (2), the production rate, normalized to the energy density of the accelerated particles is

$$q_\gamma(> E) = q_\gamma(\geq 1 \text{ TeV}) \left( \frac{E}{1 \text{ TeV}} \right)^{3-\alpha} \quad (6)$$

**Table 1.** The production rates of  $\gamma$ -rays for different spectral indices  $\alpha$  of the parent cosmic ray distributions,  $f(p) \propto p^{-\alpha}$ . The contribution of nuclei other than H in both the CR and the target matter is assumed to be the same as in the ISM, ie the pure proton contribution is multiplied by a factor 1.5 (cf Dermer, 1986). In calculating the low energy part of the production rate we used the formalism developed by Stecker (1971). The units are  $\text{s}^{-1}\text{erg}^{-1}\text{cm}^3(\text{H-atom})^{-1}$ .

$\alpha$	$q_\gamma(\geq 100 \text{ MeV})$	$q_\gamma(\geq 1 \text{ TeV})$
4.1	$0.46 \times 10^{-13}$	$1.02 \times 10^{-17}$
4.2	$0.58 \times 10^{-13}$	$4.9 \times 10^{-18}$
4.3	$0.61 \times 10^{-13}$	$2.1 \times 10^{-18}$
4.4	$0.57 \times 10^{-13}$	$8.1 \times 10^{-19}$
4.5	$0.51 \times 10^{-13}$	$3.0 \times 10^{-19}$
4.6	$0.44 \times 10^{-13}$	$1.0 \times 10^{-19}$
4.7	$0.39 \times 10^{-13}$	$3.7 \times 10^{-20}$

where  $q_\gamma(\geq 1 \text{ TeV})$  is also tabulated in Table 1 for various spectral indices  $\alpha$ .

The simplified models do not as yet include any cooling of the gas (in contrast to the hydrodynamic models of Dorfi, 1991a,b), however we do not believe that this is important for the estimates presented here. The cosmic ray energy density, because of efficient diffusion, is rather uniformly distributed inside the remnants so that clumping of the gas as a result of cooling is not likely significantly to change the results. Of course cooling does change the shock strength, and therefore the acceleration efficiency, in the late stages of SNR evolution.

To discuss the visibility of SNR as  $\gamma$ -ray sources two quantities seem most interesting. The first is the total luminosity of the remnant in photons per second, the second the surface brightness along a line through the centre of the remnant in photons  $\text{cm}^{-2} \text{s}^{-1} \text{sr}^{-1}$ . While the first measure is appropriate to discussions of the detectability of unresolved sources, the second is more appropriate for spatially resolved sources. Figure 1 shows both measures for a rather standard SNR model together with the radii of the shock, the thickness of the precursor and the partition of the explosion energy between thermal and nonthermal particles. The dotted vertical line indicates the point where the post-shock gas temperature drops below  $10^6 \text{ K}$  and cooling becomes potentially important (although as noted we have not included cooling in the present calculations). For this calculation the ejecta mass was set to  $1 M_\odot$  and the ambient density to  $0.1 \text{ cm}^{-3}$ . Alfvén heating in the precursor and diffusive coupling between the interior of the remnant and the precursor were included with parameters  $\alpha_H = 1$  and  $\alpha_C = 10$ ; the injection was parameterized by specifying that a constant fraction  $\epsilon = 10^{-3}$  of the kinetic energy dissipated in the shock was given to energetic particles capable of further acceleration. The physical processes represented by the parameters  $\epsilon$ ,  $\alpha_H$  and  $\alpha_C$  are discussed in detail in DMV. Here we note simply that the effect quantified by  $\alpha_C$  is clearly required on theoretical grounds and has been shown to be a significant effect in recent numerical studies (eg Dorfi, 1991a,b). The importance of Alfvénic effects is the subject of a recent study by Jones (1993). It is worth noting that both effects act to reduce the amount of acceleration and thus tend to decrease the  $\gamma$ -ray production.

The total gamma-ray luminosity is given by  $\int q_\gamma n E_C d^3r$  which, in the context of the simplified models, can be written as  $q_\gamma (M_1 E_{C1} + M_2 E_{C2})$  where  $M_1$  is the total mass in the precursor region,  $M_2$  that in the immediate post-shock region and  $E_{C1,2}$  are the corresponding cosmic ray energy densities. Because of diffusion across the shock the two energy densities are in fact equal,  $E_{C1} = E_{C2}$ . The common value is also not very different from  $E_{C3}$ , the energy density in the interior of the remnant, for two reasons. First, there is diffusive coupling between the acceleration region around the shock and the interior of the remnant. Secondly, if the acceleration is efficient, the cosmic rays provide a substantial, if not the dominant, part of the interior pressure and the interior of the remnant has, for dynamical reasons, to be in rough pressure equilibrium. It follows that, to order of magnitude, the cosmic ray energy density throughout the remnant and in the shock precursor is  $E_{C1} = E_{C2} \approx E_{C3} \approx 3\theta E_{SN}/4\pi R^3$  where  $\theta$  is the fraction of the total supernova explosion energy,  $E_{SN}$ , converted to cosmic ray energy and  $R$  is the remnant radius. Thus for the  $\gamma$ -ray luminosity we can estimate

$$L_\gamma = q_\gamma (M_1 + M_2) \frac{3\theta E_{SN}}{4\pi R^3} \approx \theta q_\gamma E_{SN} n \quad (7)$$

$$\approx 10^{38} \theta (E_{SN}/10^{51} \text{ erg})(n/1 \text{ cm}^{-3}) \text{ ph s}^{-1}$$

where  $n$  is the ambient density. Obviously the exact value of  $\theta$  depends on the details of the model, in particular the injection parametrization used, but clearly  $\theta < 1$  and, as discussed above, the observations appear to require  $\theta \geq 0.1$  at the point when acceleration stops and the produced cosmic rays diffuse out into the ISM. In fact for reasonably plausible injection models  $\theta$  is roughly constant throughout the Sedov phase with only a moderate dependence on external parameters such as the ambient density (Markiewicz et al, 1990). At earlier times, during the free-expansion phase, the amount of energy processed through shocks is small (almost all of the explosion energy is in the form of kinetic energy of the ejecta) and  $\theta \ll 1$ .

The calculated results agree well with this simple picture; the total luminosity is low during the free-expansion phase, but is roughly constant during the Sedov phase. The Sedov phase (or better, Sedov-like, because the models are not exact similarity solutions) starts when the amount of swept up matter is roughly equal to the ejecta mass. Typically this occurs at a radius  $O(10 \text{ pc})$  and the SNR spends most of its useful life (until the outer shock becomes weak) in this phase. Cooling of the post-shock gas is important when the post-shock temperature drops below about  $10^6 \text{ K}$ , but is not as catastrophic for these models as for pure gas models because the CR do not cool and continue to provide an internal pressure in the remnant. As long as the outer bounding shock is strong and active in accelerating particles the diffusion coefficient for cosmic rays near the shock front is very small ( $\ll R\dot{R}$  except at the highest energies). Thus the accelerated particles are confined to the remnant and only diffuse out into the ISM when the shock, either because of expansion or cooling, is no longer able to maintain the strong levels of magnetic disturbance which lead to diffusion coefficients very much smaller than those in the ambient ISM.

If the SNR is a distance  $d$  away, this translates into a flux at the earth of

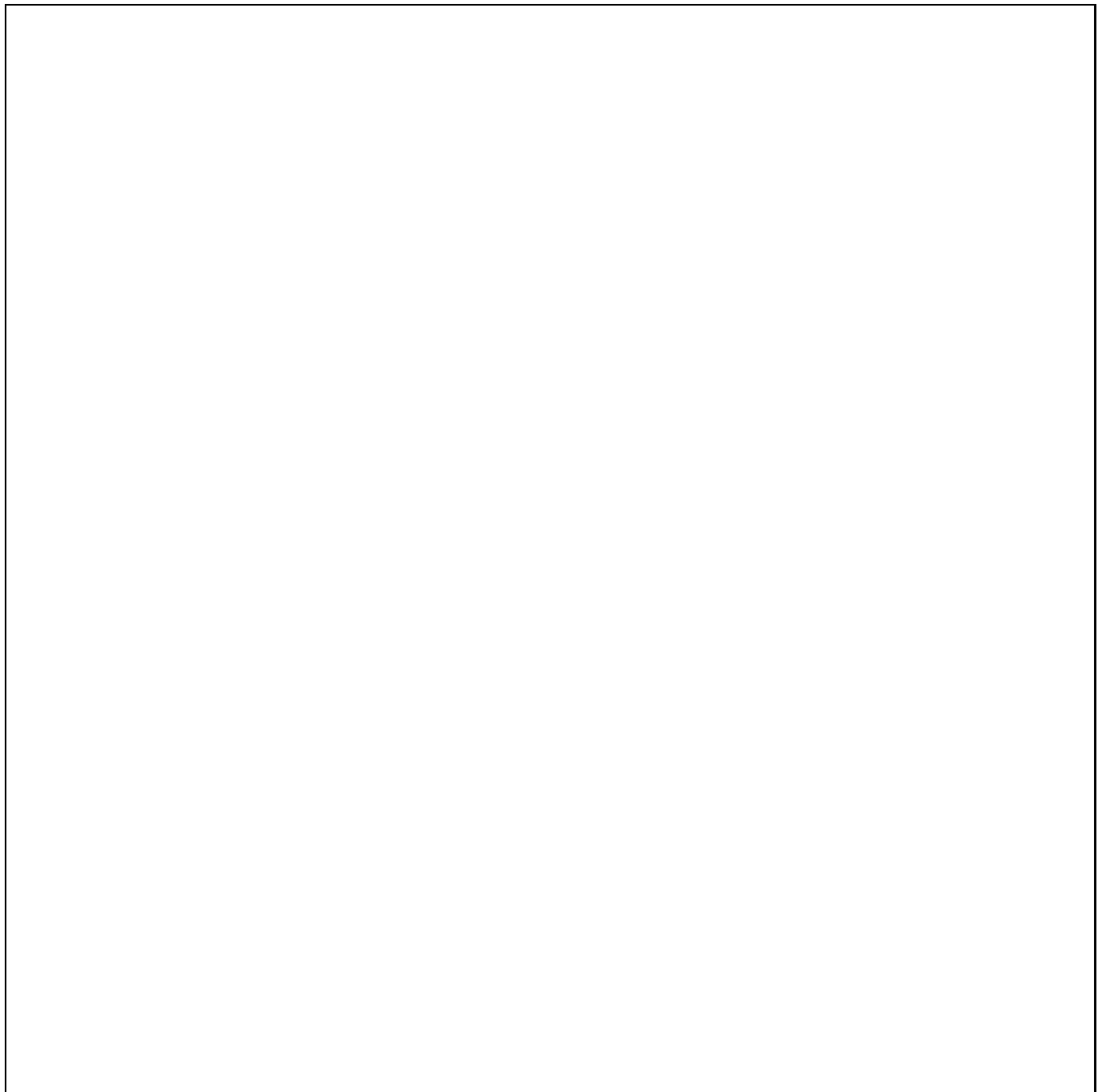


**Fig. 1.** The evolution, as a function of age in years, of the total  $\gamma$ -ray luminosity (in photons with energy above 100 MeV per second) and the central surface brightness (in photons  $\text{cm}^{-2}\text{sr}^{-1}\text{s}^{-1}$ ) together with the shock radius and the width of the precursor region (in pc) and the partition of the explosion energy between accelerated particles ( $E_C$ ) and thermal gas ( $E_G$ ) for a SNR expanding into a medium of density  $0.1 \text{ cm}^{-3}$ .

$$F(\geq 100 \text{ MeV}) \approx 4.4 \times 10^{-7} \theta \left( \frac{E_{\text{SN}}}{10^{51} \text{ erg}} \right) \left( \frac{d}{1 \text{ kpc}} \right)^{-2} \left( \frac{n}{1 \text{ cm}^{-3}} \right) \text{ cm}^{-2} \text{ s}^{-1} \quad (8)$$

$\gamma$ -rays with energies above 100 MeV. Similar estimates have been given by Dorfi (1991a,b). For the same SNR parameters, and assuming a differential energy spectrum inside the remnant

proportional to  $E^{-2.1}$  or  $\alpha = 4.1$ , the flux in the high energy  $\gamma$ -ray region is

$$F(> E) \approx 9 \times 10^{-11} \theta \left( \frac{E}{1 \text{ TeV}} \right)^{-1.1} \left( \frac{E_{\text{SN}}}{10^{51} \text{ erg}} \right) \left( \frac{d}{1 \text{ kpc}} \right)^{-2} \left( \frac{n}{1 \text{ cm}^{-3}} \right) \text{ cm}^{-2} \text{ s}^{-1} \quad (9)$$

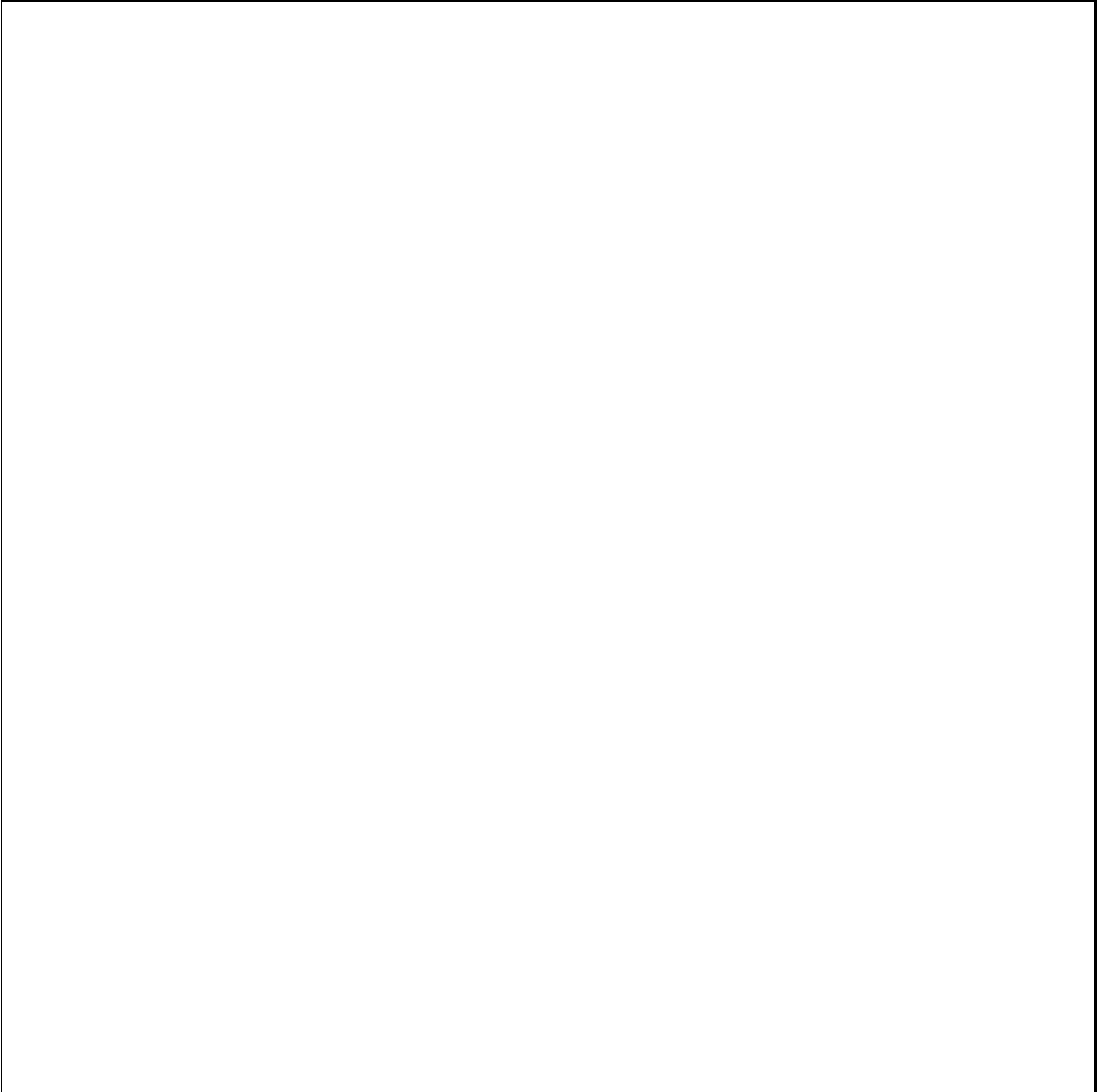


**Fig. 2.** As Fig. 1, but for an external density of  $n = 5 \text{ cm}^{-3}$ .

The surface brightness is highest approximately at the transition from the free-expansion phase to the Sedov phase. For fixed ejecta mass the radius at which this occurs scales as  $n^{-1/3}$  so that, combining this with the earlier estimate of the total luminosity, we deduce that the maximum surface brightness should scale with the external density as  $n^{5/3}$ .

In Fig. 2 results are shown for an explosion in a higher density medium with  $n = 5$  which confirm the above estimates (note that the neglect of cooling is more serious in this case). Although SNRs in denser regions of the ISM are stronger  $\gamma$ -ray sources than those in low density regions, they are probably not

as easy to detect because of the problems associated with background subtraction and source confusion. Indeed the COS-B measurements show that the diffuse  $E \geq 100 \text{ MeV}$   $\gamma$ -ray emission at  $|b| < 5^\circ$  is about  $5 \times 10^{-4}$  and  $1.5 \times 10^{-4} \text{ ph cm}^{-2} \text{ s}^{-1} \text{ sr}^{-1}$  from the inner and outer parts of the galactic plane (Bloemen, 1987). Thus the expected flux of  $\gamma$ -rays within  $1^\circ$  (the typical size of the near-by SNRs) is about  $(1.5 - 5) \times 10^{-7}$  making the detection of any source in the galactic plane with an intensity less than  $10^{-7} \text{ ph cm}^{-2} \text{ s}^{-1}$  hard even for the EGRET experiment (see Fig. 4).

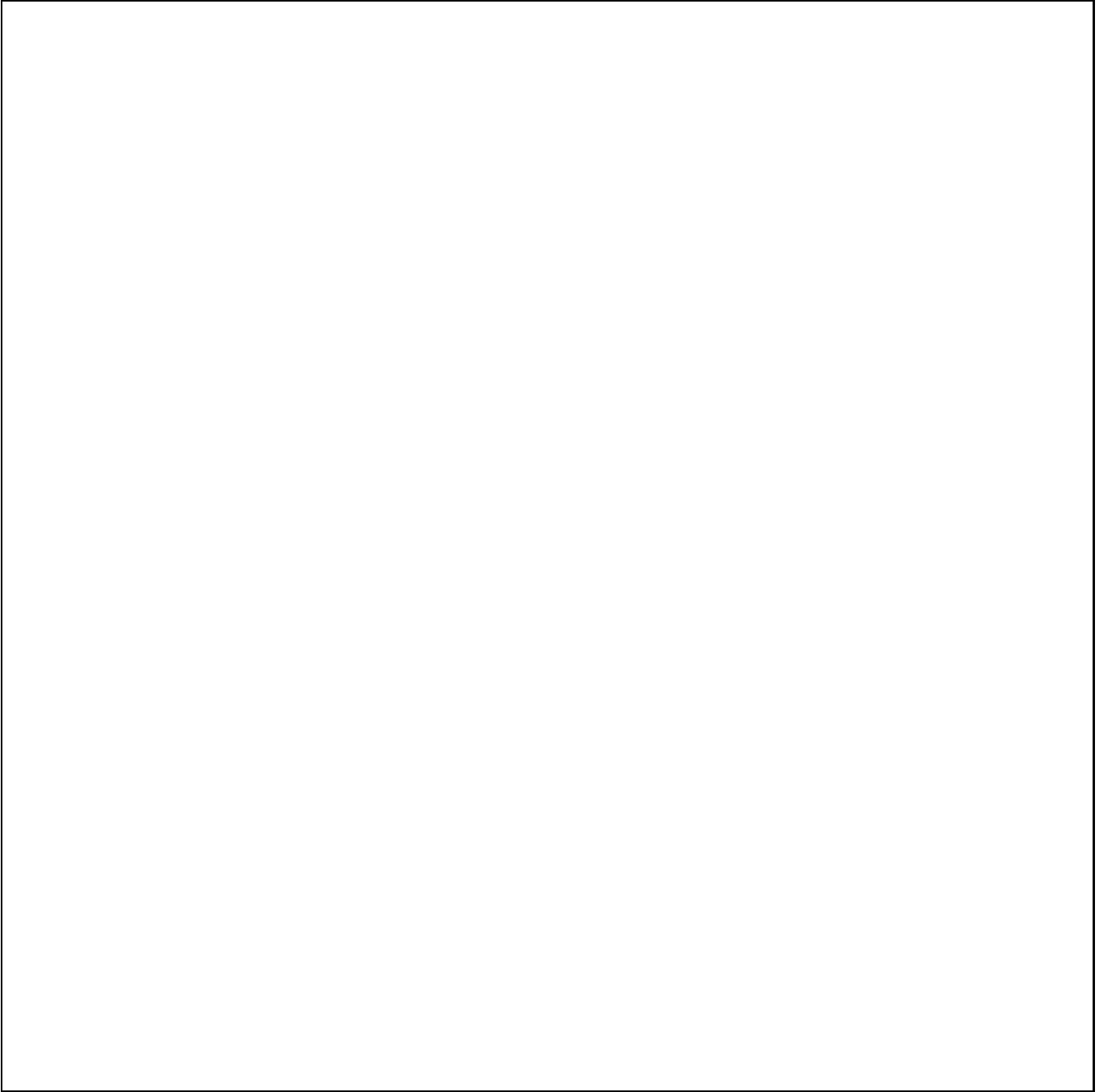


**Fig. 3.** As Fig. 1, but for an injection model which places most of the injection and acceleration at late times (see DMV for details).

It is interesting to ask whether, by allowing the injection to be weaker in strong shocks (as may be the case), it is possible to reduce the surface brightness to the point where SNRs would be hard to detect. In DMV a model of Mach number dependent injection was discussed which has the property that most of the acceleration occurs towards the end of the Sedov phase. In Fig. 3 the results for this model ( $\alpha_I = 1$  and  $\epsilon = 0$ ) are presented for  $n = 0.1$ . As expected the final total luminosity (which is determined essentially by the explosion energy and the ambient density if the acceleration is efficient) is not signif-

icantly affected, but the surface luminosity is reduced because of the larger remnant size.

Before turning to the observational implications of these models we note that they do assume expansion of the SNR into a uniform medium. While this is probably a good assumption for SNa<sub>e</sub> of type Ia, in other cases we would expect the ambient medium to be perturbed by the stellar wind and photon flux of the SN precursor. In detail this has not been explored, but qualitatively we expect that there will be rather little CR production at early times as the young SNR expands into a low-density interstellar bubble of radius  $\leq 10$  pc (although what

acceleration there is may be to energies above  $10^{14}$  eV; cf Völk and Biermann, 1988). Roughly two cases may have to be distinguished depending on the precursor star. If the SNR has swept up a wind mass which is larger or of the same amount as the SN ejecta before reaching the edge of the bubble, then the internal energy density and the pressure are roughly uniform over the SNR and therefore ‘diluted’ in the large bubble volume. With this postshock pressure the outer shock will now shock heat the ISM matter swept up and compressed by the wind (and expanding HII-region), increasing the CR production and  $L_\gamma$ . However  $\theta$  may not reach the value which would be possible if the ambient ISM had not been perturbed. In the second case, for smaller mass of the precursor star, the wind mass is considerable smaller than the ejecta mass. When the latter masses reach the edge of the bubble and shock heat the swept-up wind shell, the subsequent evolution should be very similar to that of a SNR expanding into a uniform medium. The main effect is thus probably to delay any significant CR production (and associated  $\gamma$ -ray production) until the SNR has reached the edge of the wind cavity.

### 3. Discussion

These results suggest that it should be possible to detect  $E_\gamma > 100$  MeV  $\gamma$ -rays from at least some of the relatively nearby ( $d < 1$  kpc) SNRs, especially at high galactic latitudes where the background confusion is less. It is interesting to note that claims have been made for a detection of the north polar spur (thought to be an old near-by remnant) in the COS-B and SAS-II data at flux levels similar to those discussed here, but the significance level is very low and the results depend crucially on the background subtraction model used (Lebrun and Paul, 1985; Bhat et al, 1985).

The other, perhaps more promising, possibility to test the SNR origin of cosmic rays, is to look for very high energy  $\gamma$  rays from these objects. If, as the models suggest, the accelerated particle spectra in SNRs are hard ( $\alpha \sim 4$ ) and extend to at least  $10^{14}$  eV, then the fluxes of TeV  $\gamma$ -rays expected are well above the sensitivities of modern Cherenkov telescopes, even for SNR located in low density regions of the ISM. Equation (9) shows that, for  $\theta E_{\text{SN}} = 10^{50}$  erg, the flux of TeV  $\gamma$ -rays expected from a near-by SNR (at  $d \leq 1$  kpc) exceeds  $10^{-12}$  ph cm $^{-2}$ s $^{-1}$  at  $n \geq 0.1$  cm $^{-3}$ .

Because the diffuse CR in the ISM have a softer spectrum than that expected for SNR source spectra the diffuse  $\pi^0$ -decay background should be much less of a problem at TeV energies and beyond than at 100 MeV. There is also a diffuse Galactic  $\gamma$ -ray background resulting from IC scattering of the 2.7 K cosmic microwave background by the CR electrons. But at TeV energies this also appears to be relatively less important than at  $E \approx 100$  MeV (see Appendix B).

In fact for ground-based detectors, which are the only ones available at energies  $E \geq 0.1$  TeV, the principal background flux is that of the cosmic ray electrons themselves because they produce atmospheric showers which are indistinguishable from  $\gamma$ -ray induced showers of the same primary energy<sup>2</sup>. Although the background showers induced by the nucleonic component

<sup>2</sup> Of course this is not a problem for spacecraft instruments which can reject charged particle events by using an anti-coincidence shield.

of the CR are much more frequent, it is possible to discriminate, at least partially, between hadronic and electromagnetic showers using various characteristics of the shower secondaries. At TeV energies morphological analysis of the Cherenkov light image has been shown to be a powerful technique for rejecting hadronic showers, and at  $E \geq 100$  TeV the muon content can be used. The sensitivities of modern ground-based detector systems to cosmic  $\gamma$ -ray fluxes are mainly determined by the efficiency of hadron rejection, which has to be estimated by detailed Monte Carlo simulations.

The observational possibilities for detecting  $\gamma$ -rays from SNRs are summarized in Fig. 4. At low  $\gamma$ -ray energies,  $E \geq 100$  MeV, the typical range of the diffuse COS-B fluxes from the galactic disc ( $|b| \leq 5^\circ$ ) are shown, bracketed from above by the average emission from the inner Galaxy and from below by the slightly harder average emission from the outer Galaxy (Bloemen, 1987). We plot the flux that would be observed by an instrument with an acceptance of  $1^\circ$ , roughly corresponding to the expected angular size of SNRs. The three upper curves are calculated spectra from SNR sources using our acceleration models for three source spectra,  $f(p) \propto p^{-\alpha}$  with  $\alpha = 4.1, 4.2$  and  $4.3$ , and using the emissivities from Appendix A. The spectra are normalized such that

$$A = \theta \left( \frac{E_{\text{SN}}}{10^{51} \text{ erg}} \right) \left( \frac{n}{1 \text{ cm}^{-3}} \right) \left( \frac{d}{1 \text{ kpc}} \right)^{-2} = 1 \quad (10)$$

where the quantities are as defined in section 2. For  $A \neq 1$  the plotted source spectra should be scaled by a factor  $A$ . Remarkably these curves roughly coincide at  $\gamma$ -ray energies  $\leq 1$  GeV, ie in the EGRET range.

The diffuse  $\gamma$ -ray emission, again within  $1^\circ$ , for a total hydrogen column density (both atomic and molecular)  $\langle N_{\text{H}} \rangle = \langle N_{\text{H}_2} \rangle + \langle N_{\text{HI}} \rangle = 10^{22}$  cm $^{-2}$ , a value typical of the outer Galaxy, and a cosmic ray confinement volume of size  $L = 10$  kpc, are given by the two lower curves. The curve labeled  $\pi^0$  corresponds to a diffuse Galactic cosmic ray spectrum of the form  $J_p(E) \propto (E + m_p c^2)^{-2.75}$  (see section 2)<sup>3</sup>.

The curve marked IC corresponds to the sum of the diffuse IC gamma ray emissions as discussed in Appendix B and above. Finally the background equivalence of the high energy diffuse interstellar electrons is given by the dash-dotted line, based on the observations of Nishimura et al (1980, 1990; see Appendix B).

The four hatched curve segments above 0.1 TeV correspond to the  $5\sigma$  sensitivities of different ground-based detection systems for one year of operation ( $\approx 100$  h and  $\approx 2000$  h source exposure for a single imaging telescope and charged particle detector arrays respectively). The sensitivity (defined as the minimum flux of a  $\gamma$ -ray source detectable at a level of confidence of  $m$  standard deviations) is

$$F_\gamma^{(\text{min})}(\geq E) \approx m \frac{P_{\text{CR} \rightarrow \gamma}^{1/2} S_{\text{CR}}^{1/2}}{P_{\gamma \rightarrow \gamma} S_\gamma} \left( \frac{J_{\text{CR}}(\geq E) \Delta \Omega}{t} \right)^{1/2} \quad (11)$$

<sup>3</sup> While the spectrum above 10 GeV is well determined, at lower energies, where solar modulation is dominant, we do not really know the form of the demodulated ISM spectrum. This particular form is compatible with the observations, and has been extensively used by many authors in the past (eg Stecker, 1971), but otherwise has no special significance.

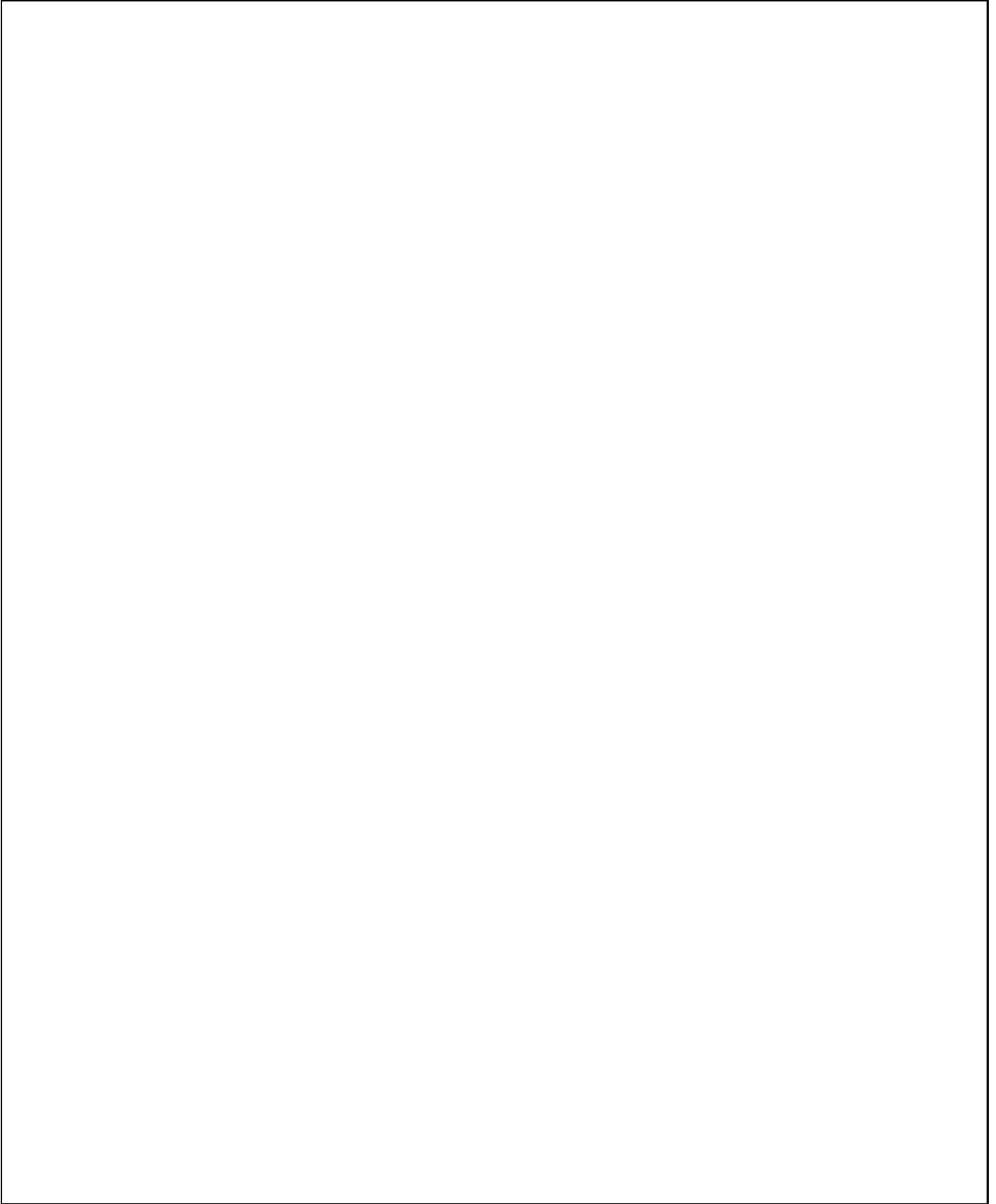


**Fig. 4.** The predicted  $\gamma$ -ray fluxes from a SNR together with the various Galactic backgrounds (for a  $1^\circ$  source) and current instrumental sensitivities; see text for details.



where  $J_{\text{CR}}(\geq E)$  is the integral cosmic ray flux,  $\Delta\Omega \approx \pi\Delta\phi^2$  where  $\Delta\phi$  is the angular resolution of the detector,  $S_\gamma$  and  $S_{\text{CR}}$  are the effective detection areas for photons and cosmic rays respectively (in general the two are not equal),  $P_{\text{CR}\rightarrow\gamma}$  is the rejection factor for background events (the probability that a CR event will be misclassified as a  $\gamma$ -ray event) and  $P_{\gamma\rightarrow\gamma}$  is the probability of correct classification of  $\gamma$ -ray induced showers. The angular and lateral distribution of the Cherenkov radiation as well as the muon content are characteristics which allow a rather efficient separation of hadronic and electromagnetic showers,  $P_{\text{CR}\rightarrow\gamma} \ll 1$  and  $P_{\gamma\rightarrow\gamma} \approx 1$  (eg Weekes, 1992). The high efficiency of the Cherenkov imaging technique has been demonstrated recently by the Whipple collaboration (Vacanti et al, 1991).

It should be noted that the detector sensitivities shown in Fig.4 correspond to point sources, namely to sources with angular size smaller than  $\Delta\phi$ , where  $\Delta\phi \simeq 0.1^\circ$  corresponds to the resolution of modern imaging Cherenkov telescopes. For extended sources the high resolution may not be of great help as far as nucleon rejection is concerned. In particular, in case of the imaging Cherenkov technique the ‘orientational’ parameters of Cherenkov images become rather ineffective, and the separation of proton- and  $\gamma$ -induced showers should be done mainly through exploiting the ‘shape’ parameters. For a single telescope, the ‘shape’ parameters alone will provide a sensitivity which is a factor 2 or 3 lower than that shown in Fig.4 (e.g. Reynolds et al, 1993). In fact, a system of imaging Cherenkov telescopes will allow a much more effective rejection of the CR background than a single telescope. The probability of detection of the  $\gamma$ -ray induced shower by a single telescope up to distances  $R \simeq 100$  m is close to 1, whereas the detection probability of CR protons near the effective energy threshold of  $\gamma$ -rays is rather low, namely  $\leq 0.1$ . Therefore the requirement of detection of a shower by a system of several ( $\geq 3$ ) telescopes, separated by 50 – 100 m from each other, practically does not reduce the number of detected  $\gamma$ -rays, but it “suppresses” the CR background by factor of at least  $10^{-2}$ , i.e. at the effective energy threshold of  $\gamma$ -rays  $S_{\text{CR}} \leq 10^{-2}S_\gamma$ . Moreover, the software analysis of the shape of the Cherenkov images in different telescopes (different projections) will be of additional help for the improvement of the efficiency of  $\gamma/p$  separation (Aharonian et al., 1993). These two factors together allow us to expect that future systems of imaging Cherenkov telescopes will approach an almost ‘background-free’ detection (i.e. the number of detected CR is smaller than the number of detected  $\gamma$ -rays) down to  $\gamma$ -ray fluxes  $F_\gamma \sim 10^{-12} \text{ ph/cm}^2 \text{ s}$ , before the statistics of  $\gamma$ -rays becomes the limiting factor, even for extended sources. Nevertheless, the angular size of the  $\gamma$ -ray sources for a reasonable value of the aperture of the imaging camera ( $\leq 5^\circ$ ) should not exceed  $\sim 2^\circ$ , since beyond  $2^\circ$  the efficiency of detection of  $\gamma$ -rays drops sharply. These results will be published elsewhere.

As we will show below the radius of a SNR only exceeds 10 pc after a minimum age of a few thousand years, provided we limit ourselves to ambient gas densities  $n \geq 0.1 \text{ cm}^{-3}$ . Obviously a SNR in a lower density environment would be very difficult to detect. Moreover for more favourable parameters, eg those characteristic of Tycho’s SNR, the time when the source size reaches 10 pc is approximately  $2 \times 10^4$  y. Note that a radius of 10 pc implies an angular size  $\leq 1^\circ$  if the source is located at more than 1 kpc. On the other hand the  $\gamma$ -ray luminosity reaches a plateau level at  $t_1 \leq 10^4$  y, and continues to be at

this level during several  $t_1$ , depending on the parameters (see Fig. 1). Since  $F_\gamma \propto L_\gamma/d^2$  the best candidates for detection are SNRs with age of order  $10^4$  years at a distance  $d \approx 1$  kpc. Of course for SNRs in dense environments the  $\gamma$ -ray fluxes may be considerable even for  $d > 1$  kpc. In galaxies similar to ours the core collapse SNe from massive stars outnumber SN type Ia by almost an order of magnitude (Evans, van den Bergh, and McClure, 1989; Tammann, 1992), and such stars form typically as clusters in dense clouds. Given the influence of these stars on the ambient medium, it is nevertheless not clear how frequent SNRs in a  $n \geq 10 \text{ cm}^{-3}$  medium are. Still, the enhanced SNR rate in the molecular ring of the Galaxy at  $d \simeq 4$  kpc (eg Bloemen et al., 1993) make this region in principle very attractive for the detection of distant SNRs. In the 100 MeV region such detection appears practically quite difficult as becomes clear from the fact that the COS-B diffuse galactic fluxes within  $1^\circ$  (a few  $10^{-7} \text{ cm}^{-2} \text{ s}^{-1}$ , see Fig. 4) approximately correspond to the sensitivity of the EGRET detector for discrete  $\gamma$ -ray sources in the galactic disc.

As can be seen from Fig. 4, the situation is better at TeV energies, where  $\gamma$ -rays from SNRs may be detected up to  $d \approx 10$  kpc provided  $n \geq 1 \text{ cm}^{-3}$ . (It is interesting to note that for SNRs with marginally detectable fluxes and angular sizes of order  $1^\circ$  a lowering of the energy threshold below 1 TeV is not necessarily the most efficient detection strategy because of the rising electron background.) Therefore future imaging Cherenkov telescopes (ICT) will be very useful in searching for high energy  $\gamma$ -rays from SNRs within wide ranges of ages and distances. The detection of near-by ( $d < 1$  kpc) SNRs is complicated by the large angular size of the sources, but, as was mentioned above, possible with arrays of ICTs. The Whipple GRANITE detector (Akerloff et al, 1990) consisting of two  $\approx 10$  m imaging telescopes has been built recently, and the HEGRA imaging telescope array (Aharonian et al, 1991) consisting of five ICTs is now under construction at La Palma. The high angular resolution of ICT arrays will allow the  $\gamma$ -ray spectrum to be measured with rather high accuracy ( $\Delta E/E \approx 20\%$ ) and thus give direct information about the spectrum of accelerated particles in the SNR. The weak dependence of the fluxes at 0.1 to 1 GeV on the shape of spectrum of accelerated particles (assuming a power-law form; see Fig. 4) means that measurements in this energy range are in some ways less informative than those at TeV energies. However, for the same reason, EGRET measurements can provide a rather model-independent estimate of the normalization parameter  $A$  [Eq. (9)] and thus the total nonthermal power of SNRs.

The important practical question of identifying candidate SNRs for observation can best be illustrated by an example. Let us consider Tycho’s SN of 1572 which is at an estimated distance of  $d = 2.25 \pm 0.25$  kpc (e.g. Heavens, 1984). From the historical light curve the SN is commonly assumed to have been of type Ia, an accreting white dwarf system, for which our model assumptions of a uniform ambient medium are probably well justified (cf the discussion at the end of section 2). According to the most recent radio observations (Tan and Gull, 1985) the expansion parameter  $t\dot{R}/R = 0.462 \pm 0.024$  where  $R(t)$  is the outer SNR radius and  $\dot{R}(t)$  its time derivative at time  $t$  after the initial explosion. Thus the expansion parameter has decreased quite far towards its asymptotic value of 0.4 in the Sedov phase. This dynamical argument is probably more reliable than present X-ray models which need to take account of non-equilibrium electron temperatures and non-equilibrium

ionisation states behind the outer shock as well as nonsolar chemical composition in the ejecta which are part heated by the reverse shock. Thus Tycho's SNR is probably quite close to the Sedov phase. Different X-ray models give results ranging from  $n = 0.28 \text{ cm}^{-3}$  and  $E_{\text{SN}} = 7 \times 10^{50} \text{ erg}$  (Hamilton et al, 1986) to  $n = 1.13 \text{ cm}^{-3}$  and  $E_{\text{SN}} = 1.9 \times 10^{50} \text{ erg}$  (Smith et al, 1988). A value of  $E_{\text{SN}}/n = 0.17 \times 10^{51} \text{ erg cm}^3$  with a quoted error of about 20% from the latter reference agrees reasonably well with the dynamical value of  $E_{\text{SN}}/n = 0.2 \times 10^{51} \text{ erg cm}^3$  inferred by Heavens (1984) from radio and X-ray data and gives the value  $nE_{\text{SN}} = 0.2 \times 10^{51} \text{ erg cm}^{-3}$ . Thus assuming  $\theta \approx 0.2$  we have  $A \approx 0.01$ . If the Sedov phase is far from being reached, then we may have  $\theta \ll 0.2$  and  $A \ll 10^{-2}$ ; however it would be hard to reconcile this with the amounts of shock heated gas seen in the X-ray band as well as the kinematical evidence from the expansion parameter. Alternatively, it may be that in this particular remnant particle acceleration is inefficient and  $\theta \ll 0.2$ ; but then, if the Galactic SNRs are the sources of the cosmic rays, the remaining SNRs must be even stronger accelerators and we soon run into energy problems. Thus, on balance, the prediction of  $A \approx 0.01$  for Tycho's SNR is a hypothesis worth testing.

The spectrum inside such a young SNR is presumably very hard with  $\alpha \leq 4.1$ . This is due to the fact that the shock is still very strong and wave heating is inefficient (DMV) so that even in a simple test particle approximation the spectrum is very hard (Völk, Zank and Zank, 1988). Nonlinear effects tend to flatten the high-energy end of the spectrum so that assuming a spectral slope of 4.1 for Tycho is not unreasonable. On looking at Fig. 4 we see that an EGRET detection of Tycho appears impossible, but that it should be visible at 1 TeV for imaging Cherenkov arrays and at 20 TeV for a  $1 \text{ km}^2$  AEROBICC array. The present radius of Tycho's SNR corresponds to about 4 arc minutes.

This situation should persist for  $10^4$  years at which epoch Tycho's SNR will have an angular radius of about  $0.25^\circ$ . The fraction of the explosion energy converted to cosmic ray energy should remain at  $\theta \approx 0.2$  or higher while the spectral slope will begin to increase from  $\alpha \approx 4.1$  to  $\alpha \approx 4.3$  only towards the end of the evolution. Therefore a remnant of this type may be better observed at somewhat later times. It is worth noting that if Tycho were located at  $d = 1 \text{ kpc}$  we would have  $A \approx 0.1$  and detection would be much simpler. Obviously SNRs in denser environments are better candidates at the same distance and comparable evolutionary epochs. But we are dealing here with the statistics of a small number of nearby sources and each candidate requires an individual evaluation before sensitive survey instruments become available.

Most models of CR acceleration in SNRs predict upper cut-offs in the spectrum between  $10^2$  and  $10^3 \text{ TeV}$ . There will however be some SNRs whose precursor stars were massive OB stars or Wolf-Rayet stars. These SNaE explode into a medium where the magnetic field is that in the wind of the progenitor star and under these circumstances energies as high as  $10^3$  or  $10^4 \text{ TeV}$  may be possible (Völk and Biermann, 1991). If such special sources have power-law spectra a clear observational test of their existence is possible with the existing UMC (Utah, Michigan, Chicago) detector (Fick et al, 1991). The  $5\sigma$  sensitivity of this system above  $100 \text{ TeV}$  at present reaches about  $3 \times 10^{-14} \text{ ph cm}^{-2} \text{ s}^{-1}$  in one year of operations (see Fig. 4). Therefore the efficiency of CR acceleration in SNR to energies

significantly above  $10^3 \text{ TeV}$  may soon be tested for all near-by SNRs using the all sky survey of the UMC detector.

The new generation air shower detectors like CRT (the Cosmic Ray Tracking experiment; Heintze et al, 1989) MILAGRO (Multiple Image Los Alamos Gamma Ray Observatory; Williams et al 1991) and the  $1 \text{ km}^2$  AEROBICC (AIR shower Observation By angle Integrating Cherenkov Counters; Lorenz, 1992) could observe SNR sources above  $10 \text{ TeV}$  provided the source CR spectra extend to energies  $\geq 10^2 \text{ TeV}$  (note that the spectra in Fig. 4 have been drawn with no high energy cutoff). Thus even negative results, in the form of firm upper limits in the  $E \geq 10 \text{ TeV}$  range, could be of great importance in determining the upper cutoff of the acceleration process in SNRs.

Although this paper concentrates, for obvious reasons, on the  $\gamma$ -ray visibility, there is another possibility to detect high energy stable neutral particles from SNRs. From Table A1 we expect (for hard source spectra,  $\alpha \approx 2$ ) a neutrino flux above  $1 \text{ TeV}$  of

$$F_{\nu\mu}(\geq 1 \text{ TeV}) \approx 10^{-10} A \text{ neutrinos cm}^{-2} \text{ s}^{-1} \quad (12)$$

Such fluxes may be marginally detectable for DUMAND (Deep Underwater Muon And Neutrino Detector; eg Okada, 1991) in the case of near-by SNRs. This is especially interesting because of the all sky survey capability of DUMAND.

Besides SNRs in our own Galaxy, it may be possible to use the same combination of techniques to detect the integrated  $\gamma$ -ray flux of some favourable near-by normal galaxies. Such galaxies do not have an active nucleus, but presumably contain the same types of cosmic ray sources as our Galaxy. Examples might be the Magellanic Clouds and the near-by starburst galaxy M82. This will be discussed in a separate paper.

#### 4. Summary

Recent nonlinear particle acceleration models for SNRs have been used to predict their  $\gamma$ -ray luminosities. A detailed analysis of the various backgrounds shows that the most favourable energy range for detecting  $\gamma$ -rays from SNRs is probably from  $1$  to  $10 \text{ TeV}$ . In addition, to characterise the spectra, detections in the GeV region and detections or upper bounds in the PeV region would be very useful and appear possible with current detectors.

Galactic SNRs should be detectable  $\gamma$ -ray sources at distances of up to a few kpc in regions of the ISM where the mean density is of order  $1 \text{ cm}^{-3}$  or more, if, as is generally supposed, they are the main sources of the cosmic rays below  $10^{14}$  to  $10^{15} \text{ eV}$ . Even the detection of one or two SNR which are not dominated by a pulsar, at the level suggested in this paper would be a convincing demonstration of the SNR origin of cosmic rays.

*Acknowledgements.* Various aspects of this work were discussed at meetings in Vulcano and Ringberg. The authors are especially indebted to E.Dorfi, A.Heavens,R.Tuffs, and R.Wielebinski for helpful remarks, and to P.O.Lagage for critical comments on manuscript.

## References

- Aharonian F A, Akhperjanian A G, Kankanian R S, Mirzoyan R G, Samorski M, Stamm W, Bott-Bodenhausen M, Lorenz E, Sawallisch P, 1991, Proposal for Imaging Air Cherenkov Telescopes in the HEGRA Particle Array, Kiel
- Aharonian F A, Chilingarian A A, Mirzoyan R G, Konopelko A K, Plyaskeshnikov A V, 1993, *Experimental Astronomy* (in press)
- Aharonian F A, 1991, *Ap&SS* 180, 305
- Akerlof CW, Cawley M F, Feegan D J, Hillas A M, Lamb R C, Lewis D A, Meyer D I, Weekes T C, 1990, *Nucl. Phys. B (Proc. Suppl.)* 14A, 237
- Berezhko E G, Krymsky G F, 1988, *Usp. Fiz. Nauk.* 154, 49 (English translation, *Sov. Phys. Usp.* 31, 27)
- Bhat et al, 1985, *Nature* 314, 515.
- Blandford R D, Eichler D, 1987, *Phys. Rep.* 154, 1
- Blandford R D, Ostriker J P, 1980, *ApJ* 237, 793
- Bloemen J B G M, 1987, *ApJ*, 317, L15
- Bloemen, J B G M, Dogiel, V A, Dorman V L, Ptuskin V S, 1993, *A&A* 267, 372
- Blumenthal G R, Gould R J, 1970, *Rev. Mod. Phys.* 72, 237
- Bogdan T, Völk H J, 1983, *A&A* 122, 129
- Cronin J W, 1992, *Nucl. Phys. B (Proc. Suppl.)* 25A, 137
- Dermer C D, 1986, *A&A* 157, 223
- Dorfi E A, 1990, *A&A* 234, 419
- Dorfi E A, 1991a, *Proc 22nd ICRC (Dublin)* 1, 109
- Dorfi E A, 1991b, *A&A* 251, 597
- Drury L O'C, Markiewicz W J, Völk H J [DMV], 1989, *A&A* 225, 179
- Evans R S, van den Bergh S, McClure R D, 1989. *ApJ* 345, 752
- Fick B E, Borione A, Covault C E, Cronin J W, Gibbs H A, Krimm H A, Mascarenhas N C, McKay T A, Muller D, Newport B J, Ong R A, Rosenberg B J, 1991, *Proc 22 ICRC (Dublin)* 2, 728
- Gaisser T K, 1990, *Cosmic Rays and Particle Physics*, Cambridge University Press, Cambridge.
- Hamilton A J S, Sarazin C L, Symkowiak A E, 1986, *ApJ* 300, 713
- Heavens A F, 1984, *MNRAS* 211, 195
- Heintze J et al, 1989, *Nuc. Instr. and Methods* A227, 29
- Higdon J C, Lingenfelter R E, 1975, *Astrophys. J.* 198, L17
- Jokipii J R, Ko M, 1987, *Proc 20 ICRC (Moscow)* 2, 179
- Jones L W, 1990, *Proc 21st ICRC (Adelaide)* 2, 75
- Jones T W, 1993, *ApJ* (submitted)
- Juliusson E, Meyer P, Müller D, 1972, *Phys. Rev. Lett.* 21, 445
- Kang H, Drury L O'C, 1992, *ApJ* 399, 182
- Kang H, Jones T W, 1991, *MNRAS* 249, 439
- Krymsky G F, Petukhov S I, 1980, *Pis'ma Astron. Zh.* 6, 227 (English translation, *Sov. Astron. Lett.* 6, 124)
- Lagage P O, Cesarsky C J, 1983, *A&A* 125, 249
- Lebrun F, Paul J, 1985, *Proc 19 ICRC (la Jolla)* 1, 309.
- Lorenz E, 1992, Presentation at the Paris workshop on VHE  $\gamma$ -ray detectors
- Markiewicz W J, Drury L. O'C., Völk H J, 1990, *A&A* 236, 487
- Moraal H, Axford W I, 1983, *A&A* 125, 204
- Nishimura J, Fujii M, Taira T, Aizu E, Hiraiwa H, Kobayashi T, Niu K, Ohta I, Golden R L, Koss T A, Lord J J, Wilkes R J, 1980, *ApJ* 238, 394
- Nishimura J, Fujii M, Kobayashi T, Aizu H, Komori Y, Kazuno M, Taira T, Koss T A, Lord J J, Wilkes R J, Woosley J, 1990, *Proc 21st ICRC (Adelaide)* 3, 213.
- Okada A, 1991, in: *Astrophysical Aspects of the Most Energetic Cosmic Rays*, eds. Nagano M and Takahara F, World Scientific, Singapore, p.483
- Prischep V L, Ptuskin V S, 1981, *Astron. Zh.* 58, 779 (English translation, *Sov. Astron.* 25, 446)
- Reynolds P T, Akerlof C.W., Cawley M F, Chantel M, Fegan D J, Hillas A M, Lamb R C, Lang M J, Lawrence M A, Lewis D A, Macomb D, Meyer A I, Mohanty G, O'Flaherty K S, Punch M, Schubnell M S, Vacanti G, Weekes T C, Whitaker T, 1993, *ApJ* 404, 206
- Smith A, Davelaar J, Peacock A, Taylor B G, Morini N, Robba N R, 1988 *ApJ* 325, 288
- Stecker F W, 1971, *Cosmic Gamma Rays (NASA Scientific and Technical Information Office)*, NASA SP-249.
- Stecker F W, 1979, *ApJ* 228, 919
- Swordy S P, Müller D, Meyer P, L'Heureux J, Grunsfeld J M, 1990, *ApJ* 349, 625
- Tammann G A, 1992, in: *Supernovae*, Bludman S, Mochkovitch R and Zinn-Justin (eds.), Les Houches, Elsevier Science Publishers B.V., p.1
- Tan S M, Gull S F, 1985, *MNRAS* 216, 949
- Vacanti G, Cawley M F, Colombo E, Fegan D J, Hillas A M, Kwok P W, Lang M J, Lamb R C, Lewis D A, Macomb D J, O'Flaherty K S, Reynolds P T, Weekes T C, 1991, *ApJ* 377, 467
- Völk H J, Biermann P L, 1988, *ApJ* 333, L65
- Völk H J, Drury L O'C, Dorfi E A, 1985, *Proc 19th ICRC (La Jolla)* 3, 148
- Völk H J, Zank L, Zank G, 1988, *A&A* 188, 274
- Weekes T, 1992, *Space Sci. Rev.* 59, 315
- Williams D A, et al, 1991, *Proc 22nd ICRC (Dublin)* 2, 684

## Appendix A: The emissivity of very high energy neutral particles in p-p interactions

On the assumption that the primary protons have a power-law differential energy spectrum,

$$N_p(E) = N_0 E^{-\alpha+1}, \quad A1$$

the emissivity for the secondary particles produced in p-p interactions may be written in the form

$$\mathcal{E}_S(E) = \langle mx \rangle_S^\alpha \sigma_{pp} c N_p(E) \quad A2$$

where  $\sigma_{pp}$  is the inelastic p-p cross-section,  $c$  is the velocity of light and

$$\langle mx \rangle_S^\alpha = \int_0^1 x^\alpha g(x) dx \quad A3$$

is the so-called spectrum-weighted moment of the inclusive cross-section (see, e.g. Gaisser 1990;  $x$  is the ratio of the secondary particle energy to that of the primary proton and  $g(x)$  is the dimensionless inclusive cross-section).

A comprehensive discussion of the spectrum-weighted moments for secondary hadrons based on the interaction of accelerator beams with fixed targets at beam energies  $\leq 1$  TeV has been presented by Gaisser (1990). In table A1 we present

the spectrum-weighted moments for  $\pi^0$ -mesons from Gaisser's book.

As the production and decay of secondary  $\pi^0$  mesons is the main source of  $\gamma$ -rays (the contribution from the next most important channel via  $\eta$  mesons is only about  $\langle mx \rangle_\eta / \langle mx \rangle_{\pi^0} \approx (m_{\pi^0}/m_\eta)^2 \approx 0.06$ )

$$\mathcal{E}_\gamma(E) = 2 \int_E^\infty \frac{\mathcal{E}_{\pi^0}(E')}{E'} dE' = \frac{2}{\alpha+1} \mathcal{E}_{\pi^0}(E) \quad A4$$

and thus

$$\langle mx \rangle_\gamma^\alpha \approx \langle mx \rangle_{\pi^0}^\alpha \frac{2}{\alpha+1} \quad A5$$

Though the values of  $\langle mx \rangle_{\pi^0}$  given in Table A1 are calculated for fixed target accelerator data with  $E \leq 1$  TeV it is expected that they correctly characterise also the energy region beyond 1 TeV (Gaisser, 1990). Indeed, the spectrum-weighted moments for gamma rays calculated on the basis of data from p- $\bar{p}$  colliders at  $\sqrt{s} = 630$  GeV (the CERN UA7 experiment) can be approximated in simple form (A. Erlykin, personal communication) by

$$\log \langle mx \rangle_\gamma^\alpha = 1.49 - 2.73\alpha + 0.53\alpha^2 \quad A6$$

Comparison of Eq. A6 with  $\langle mx \rangle_\gamma^\alpha \approx \langle mx \rangle_{\pi^0}^\alpha \frac{2}{\alpha+1}$  and the values of  $\langle mx \rangle_{\pi^0}^\alpha$  in Table A1 shows agreement within 20%, which seems very reasonable if account is taken of the uncertainty associated with the contribution through  $\eta$ -mesons, especially at high energies.

**Table A1.** Spectrum weighted moments for the production of secondaries in p-p collisions.

$\alpha$	1.0	1.2	1.4	1.6	1.8
$\langle mx \rangle_\gamma^\alpha$ Eq. (6)	0.19	0.094	0.051	0.030	0.019
$\langle mx \rangle_{\pi^0}^\alpha$ Gaisser (1990)	0.17	0.092	0.066	0.048	0.036
$\langle mx \rangle_n^\alpha$ Eq. (11) Gaisser (1990)	0.062	0.050	0.041	0.034	0.029
$\frac{\gamma}{\nu_\mu + \nu_\mu}$ Eq. (9, 10) Gaisser (1990)	0.95	0.80	0.67	0.56	0.46
	0.98	0.86	0.77	0.66	0.58

At p-p interactions, as a result of the decay of charged pions, neutrinos will also be produced. From the point of view of detectability the most interesting are the muonic neutrinos,  $\nu_\mu$  and  $\bar{\nu}_\mu$ , produced in the decays (1)  $\pi^\pm \rightarrow \mu^\pm + \nu_\mu$  and (2)  $\mu^\pm \rightarrow e^\pm + \nu_\mu + \nu_e$ . Taking into account that

$$\mathcal{E}_{\pi^0} \approx \frac{1}{2} \mathcal{E}_{\pi^\pm} \quad A7$$

and the relation (eg Stecker, 1979)

$$\mathcal{E}_\mu^{(1)}(E) = \frac{1}{2\eta} \int_{E/2\eta}^\infty \frac{\mathcal{E}_{\pi^\pm}(E')}{E'} dE' = \frac{(2\eta)^\alpha}{\alpha+1} \mathcal{E}_{\pi^\pm}(E) \quad A8$$

gives for the first decay

$$\mathcal{E}_{\nu_\mu}^{(1)}/\mathcal{E}_\gamma = (2\eta)^\alpha \quad A9$$

where  $\eta = 1 - m_\mu^2/m_\pi^2$ . An exact calculation of the  $\nu_\mu$  spectrum from decay (2) is more complicated, however it can be estimated as follows. In charged pion decays on average a fraction  $(1 - \eta)$  of the pion energy is transferred to the muons, while approximately the same ( $\approx 1/3$ ) part of the muon energy goes to the decay products,  $e^\pm$ ,  $\nu_\mu$  and  $\nu_e$ . Thus in this simple approximation

$$\mathcal{E}_{\nu_\mu}^{(2)}/\mathcal{E}_\gamma \approx (\alpha+1)\xi^\alpha; \quad \xi = \frac{1-\eta}{3} \approx 0.026 \quad A10$$

Equations A10 and A9 imply that both channels (1) and (2) make comparable contributions to the  $\nu_\mu$  production rate and that for hard proton spectra ( $\alpha \approx 1$ ) the ratio of gamma to neutrino production is close to unity.

Over distances of order  $(E/10^{17} \text{ eV}) \text{ kpc}$  neutrons can also be considered as quasistable neutral particles of possible astrophysical interest. The emissivity of neutrons can be calculated using the mean neutron multiplicity  $\langle m \rangle \approx 1/4$  and the normalised  $x$ -distribution of neutrons,  $g(x) = 3(1-x)^2$ , suggested by Jones (1990) with the result

$$\langle mx \rangle_n^\alpha = \frac{3}{4} \frac{\Gamma(3)\Gamma(\alpha+1)}{\Gamma(\alpha+3)} = \frac{3}{2} \frac{1}{(\alpha+3)(\alpha+2)(\alpha+1)} \quad A11$$

The various spectrum-weighted moments for stable neutral particles are presented in Table A1.

## Appendix B: The diffuse Galactic $\gamma$ -ray emission at very high energies

The Galactic  $\gamma$ -ray background consists of two components,  $\pi^0$  and IC, resulting from interactions of cosmic ray nucleons and electrons with the ISM. The flux of the first component can be presented in the form (Aharonian, 1991)

$$J_\gamma^{\pi^0} = \frac{1}{4\pi} \mathcal{E}(> E) \eta \langle N_H \rangle = \langle mx \rangle_\gamma^\alpha \sigma_{pp} \eta J_{CR}(> E) \langle n_H \rangle \quad B1$$

where  $\sigma_{pp}$  is the inelastic p-p cross-section,  $\langle mx \rangle_\gamma^\alpha$  is the spectrum weighted moment for  $\gamma$ -rays (see Appendix A),  $J_{CR}(> E)$  is the integral energy spectrum of the Galactic cosmic rays,  $\eta$  is the contribution of nuclei, mostly  $^4\text{He}$ , in the cosmic rays and the ISM to  $\pi^0$  production (for standard composition  $\eta \approx 1.5$ , see eg Dermer, 1986) and  $\langle N_H \rangle = \langle N_{\text{HI}} \rangle + \langle N_{\text{H}_2} \rangle$  is the total hydrogen (atomic and molecular) column density in the given direction.

Radio measurements in the 21 cm and 2.6 mm lines provide rather accurate estimates of  $\langle N_H \rangle$ , so the main uncertainty is associated with the cosmic ray flux above 1 TeV. Indeed, if the CR proton spectrum is taken to be

$$J_{CR}(> E) \approx 7 \times 10^{-6} \left( \frac{E}{1 \text{ TeV}} \right)^{-1.75} \text{ cm}^{-2} \text{ s}^{-1} \text{ sr}^{-1} \quad B2$$

then at  $E \gg 100$  MeV we have

$$J_\gamma(> E) \approx 1.2 \times 10^{-10} \left( \frac{E}{1 \text{ TeV}} \right)^{-1.75} \langle N_H \rangle_{22} \text{ cm}^{-2} \text{ s}^{-1} \text{ sr}^{-1} \quad B3$$

whereas for the Hillas (1981) representation of the spectrum,

$$J_{\text{CR}}(> E) \approx 10^{-5} \left( \frac{E}{1 \text{ TeV}} \right)^{-1.6} \text{ cm}^{-2} \text{ s}^{-1} \text{ sr}^{-1} \quad \text{B4}$$

the corresponding diffuse  $\gamma$ -ray spectrum is

$$J_{\gamma}(> E) \approx 2.2 \times 10^{-10} \left( \frac{E}{1 \text{ TeV}} \right)^{-1.6} \langle N_H \rangle_{22} \text{ cm}^{-2} \text{ s}^{-1} \text{ sr}^{-1} \quad \text{B5}$$

where  $\langle N_H \rangle_{22} = \langle N_H \rangle / 10^{22} \text{ cm}^{-2}$ . Thus there is about a factor two uncertainty in the  $\gamma$ -ray flux above 1 TeV associated with uncertainty in the Galactic CR flux.

The flux related to the electron component of the CR is even less certain. However the observations reported by Nishimura et al (1980, 1990) do extend to energies slightly above 1 TeV and show that the flux of high energy electrons is reasonably represented by a power-law,

$$J_e(E) = 7.6 \times 10^{-9} \left( \frac{E}{1 \text{ TeV}} \right)^{-3.3} \text{ cm}^{-2} \text{ s}^{-1} \text{ sr}^{-1} \text{ TeV}^{-1} \quad \text{B6}$$

in the region  $10 \text{ GeV} < E < 1 \text{ TeV}$ . Here we will assume that this spectrum extends to well above 1 TeV.

Although at 100 MeV the contributions from bremsstrahlung and IC processes on starlight and 2.7 K cosmic microwave background (CMB) are comparable, at VHE ( $E \geq 1 \text{ TeV}$ ) only IC on the CMB remains important because for  $\gamma$ -ray energies  $E \ll 4m_e^2 c^4 / 3kT \approx 10^3 \text{ TeV}$  it works in the Thomson limit and produces a hard spectrum of  $\gamma$ -rays. The emissivity of this process in the case of a narrow-spectrum background photon field with an average photon energy  $w_0$  and number density  $n_0$  is (see, eg, Blumenthal and Gould, 1970)

$$\mathcal{E}_{\gamma}^{\text{IC}} = \pi r_0^2 c n_0 N_0 2^{\beta+3} \frac{\beta^2 + 4\beta + 11}{(\beta + 3)(\beta + 1)(\beta + 5)} \left( \frac{w_0}{m_e c^2} \right)^{\frac{\beta-1}{2}} \left( \frac{E}{m_e c^2} \right)^{-\frac{\beta+1}{2}} \quad \text{B7}$$

where

$$N_e(E) = \frac{4\pi}{c} J_e(E) = N_0 E^{-\beta} \quad \text{B8}$$

is the spectrum of the relativistic electrons.

Thus, for IC of the high energy cosmic ray electrons on the CMB with  $w_0 \approx 3kT$  and  $n_0 \approx 400 \text{ cm}^{-3}$  we have

$$J_{\text{CMB}}^{\text{IC}}(> E) = \frac{1}{4\pi} \mathcal{E}_{\text{CMB}}^{\text{IC}}(> E) L_e \approx 4 \times 10^{-11} \left( \frac{E}{1 \text{ TeV}} \right)^{-1.15} \left( \frac{L_e}{10 \text{ kpc}} \right) \text{ cm}^{-2} \text{ s}^{-1} \text{ sr}^{-1} \quad \text{B9}$$

where  $L_e$  is the characteristic size of the confinement region of CR electrons in the Galaxy (in the given direction).

Equation B7 shows that, in the Thomson limit,

$$\mathcal{E}_{\gamma}^{\text{IC}} \propto n_0 w_0^{\frac{\beta-1}{2}} \propto W_0 w_0^{\frac{\beta-3}{2}} \quad \text{B10}$$

where  $W_0 = n_0 w_0$  is the energy density of the photon field. Let us consider in this limit the IC emissivities for scattering the CMB, optical and far IR radiation fields. The optical radiation, with a mean photon energy of 1.5 eV is estimated to have an energy density of  $0.5 \text{ eV cm}^{-3}$  and the far IR with a mean photon energy of 0.01 eV to have an energy density of  $0.2 \text{ eV cm}^{-3}$ . Then in the Thomson limit

$$\mathcal{E}_{\text{CMB}}^{\text{IC}} \approx 0.15 \mathcal{E}_{\text{O}}^{\text{IC}}, \quad \mathcal{E}_{\text{CMB}}^{\text{IC}} \approx 0.5 \mathcal{E}_{\text{IR}}^{\text{IC}} \quad \text{B11}$$

so that the  $\gamma$ -ray background due to the IC scattering of optical photons is roughly three times that due to the scattering of far IR photons which in turn is about twice that due to scattering of the CMB photons. However, the parameter  $\delta = E_{\gamma} w_0 / m_e^2 c^4$  is  $\approx 6(E_{\gamma}/1 \text{ TeV})$  for optical photons and  $\approx 0.04(E_{\gamma}/1 \text{ TeV})$  for IR photons. The Thomson cross-section,  $\sigma_{\text{T}}$ , is only appropriate for  $\delta \ll 1$  and for  $\delta \geq 0.01$  the Klein-Nishina cross-section,  $\sigma_{\text{KN}}$ , must be used. Asymptotically

$$\frac{\sigma_{\text{KN}}}{\sigma_{\text{T}}} = \begin{cases} 1 - 2\delta^{1/2} & \text{if } \delta \ll 1 \\ \frac{3}{8}\delta^{-1/2} [1 + \ln(2\delta^{1/2})] & \text{if } \delta \gg 1 \end{cases} \quad \text{B12}$$

so that the cross-section drops by a factor of two at  $\delta \approx 0.05$  and by more than a factor 10 at  $\delta \approx 5$ . Thus at 1 TeV and above the dominant contribution to the IC background is in fact the component produced by the CMB (the spectra also steepen in the Klein-Nishina region).

It is also easy to show that the electron bremsstrahlung contribution is negligible when compared to the IC and  $\pi^0$  backgrounds,

$$J_{\gamma}(> E) \approx 3.8 \times 10^{-13} \left( \frac{E}{1 \text{ TeV}} \right)^{-2.3} \langle N_H \rangle_{22} \text{ cm}^{-2} \text{ s}^{-1} \text{ sr}^{-1} \quad \text{B13}$$

Finally, it is interesting to note that for reasonable confinement regions,  $L_e \approx 10 \text{ kpc}$ , the ratio of the flux of IC  $\gamma$ -rays from the CMB to the primary electron flux is

$$\frac{J_{\gamma}^{\text{IC}}(> E)}{J_e(> E)} \approx 0.012 \left( \frac{E}{1 \text{ TeV}} \right)^{1.15} \quad \text{B14}$$

which is less than unity for  $E < 40 \text{ TeV}$ . In fact this ratio is only an upper limit because Klein-Nishina effects become important for IC on the CMB at about 40 TeV (see above).